

# Protection against methylglyoxal-derived AGEs by regulation of glyoxalase 1 prevents retinal neuroglial and vasodegenerative pathology

A. K. Berner · O. Brouwers · R. Pringle · I. Klaassen · L. Colhoun · C. McVicar · S. Brockbank · J. W. Curry · T. Miyata · M. Brownlee · R. O. Schlingemann · C. Schalkwijk · A. W. Stitt

Received: 19 September 2011 / Accepted: 7 November 2011 / Published online: 6 December 2011  
© Springer-Verlag 2011

## Abstract

**Aims/hypothesis** Methylglyoxal (MG) is an important precursor for AGEs. Normally, MG is detoxified by the glyoxalase (GLO) enzyme system (including component enzymes GLO1 and GLO2). Enhanced glycolytic metabolism in many cells during diabetes may overpower detoxification capacity and lead to AGE-related pathology. Using a transgenic rat model that overexpresses *GLO1*, we investigated if this enzyme can inhibit retinal AGE formation and prevent key lesions of diabetic retinopathy. **Methods** Transgenic rats were developed by overexpression of full length *GLO1*. Diabetes was induced in wild-type (WT) and *GLO1* rats and the animals were killed after 12 or 24 weeks of hyperglycaemia.  $N^{\epsilon}$ -(Carboxyethyl)lysine (CEL),  $N^{\epsilon}$ -(carboxymethyl)lysine (CML) and MG-derived-

hydroimidazalone-1 (MG-H1) were determined by immunohistochemistry and by ultra-performance liquid chromatography tandem mass spectrometry (UPLC-MSMS). Müller glia dysfunction was determined by glial fibrillary acidic protein (GFAP) immunoreactivity and by spatial localisation of the potassium channel Kir4.1. Acellular capillaries were quantified in retinal flat mounts.

**Results** *GLO1* overexpression prevented CEL and MG-H1 accumulation in the diabetic retina when compared with WT diabetic counterparts ( $p < 0.01$ ). Diabetes-related increases in Müller glial GFAP levels and loss of Kir4.1 at the vascular end-feet were significantly prevented by *GLO1* overexpression ( $p < 0.05$ ) at both 12- and 24-week time points. *GLO1* diabetic animals showed fewer acellular capillaries than WT diabetic animals ( $p < 0.001$ ) at 24 weeks' diabetes.

A.K. Berner, O. Brouwers and R. Pringle contributed equally to this study.

**Electronic supplementary material** The online version of this article (doi:10.1007/s00125-011-2393-0) contains peer-reviewed but unedited supplementary material, which is available to authorised users.

A. K. Berner · R. Pringle · L. Colhoun · C. McVicar · S. Brockbank · J. W. Curry · A. W. Stitt (✉)  
Centre for Vision and Vascular Science, Queen's University Belfast, Royal Victoria Hospital, Belfast BT12 6BA, Northern Ireland, UK  
e-mail: a.stitt@qub.ac.uk

O. Brouwers · C. Schalkwijk  
Department of Internal Medicine, Universiteit Maastricht, Maastricht, the Netherlands

T. Miyata  
United Centers for Advanced Research and Translational Medicine (ART), Tohoku University Graduate School of Medicine, Miyagi, Japan

I. Klaassen · R. O. Schlingemann  
Department of Ophthalmology, Academic Medical Center, University of Amsterdam, Amsterdam, the Netherlands

R. O. Schlingemann  
Department of Clinical and Molecular Ophthalmogenetics, The Netherlands Institute for Neuroscience, Royal Netherlands Academy of Arts and Sciences (KNAW), Amsterdam, the Netherlands

M. Brownlee  
Einstein Diabetes Research Center, Albert Einstein College of Medicine, New York, NY, USA

**Conclusions/interpretation** Detoxification of MG reduces AGE adduct accumulation, which, in turn, can prevent formation of key retinal neuroglial and vascular lesions as diabetes progresses. MG-derived AGEs play an important role in diabetic retinopathy.

**Keywords** AGEs · Diabetic complications · Diabetic retinopathy · Glyoxalase 1 · Methylglyoxal · Pathogenesis · Retina

### Abbreviations

3-DG	3-Deoxyglucosone
AR	Aldose reductase
CEL	<i>N</i> <sup>ε</sup> -(Carboxyethyl)lysine
CML	<i>N</i> <sup>ε</sup> -(Carboxymethyl)lysine
GFAP	Glial fibrillary acidic protein
GLO	Glyoxalase
GO	Glyoxal
GSH	Glutathione
MG	Methylglyoxal
MG-H1	MG-derived-hydroimidazolone-1
RAGE	Receptor for AGEs
UPLC-MSMS	Ultra-performance liquid chromatography tandem mass spectrometry
WT	Wild-type

### Introduction

Diabetic retinopathy is a complex condition with a multifactorial pathogenesis. Among several hyperglycaemia-mediated pathogenic mechanisms that may contribute to this diabetic complication is the formation and accumulation of AGEs [1]. Clinical studies have demonstrated that serum levels of *N*<sup>ε</sup>-(carboxy-methyl)lysine (CML), pentosidine and methylglyoxal (MG)-derived hydroimidazolone-1 (MG-H1) are associated with disease progression [2–4]. However, serum AGEs can be variable and evidence suggests that intracellular and matrix-immobilised AGEs are more robust biomarkers [1]. For example, Genuth et al. have demonstrated that crosslinking AGEs on long-lived skin proteins are significantly associated with progression of diabetic retinopathy [5]. Beyond clinical correlates, AGEs and related advanced lipoxidation end-products (ALEs) accumulate in the retinal vasculature and Müller glia during diabetes [6–8], and AGE inhibitors show efficacy in reducing retinal lesions in diabetic animal models [8–11].

AGEs can form directly from the reaction of glucose with amino groups or from the reaction with  $\alpha$ -oxoaldehydes such as glyoxal (GO), MG and 3-deoxyglucosone (3-DG). These highly reactive intermediates arise from both chemical and metabolic pathways and can lead to rapid adduct formation on lysine and arginine residues [12].  $\alpha$ -Oxoaldehydes occur at

elevated levels in cells exposed to high glucose and also in diabetic serum, and are probably the most important source of intra- and extracellular AGEs [13, 14]. For example, MG can give rise to *N*<sup>ε</sup>-(carboxyethyl)lysine (CEL), argpyrimidine and MG-H1, which have been identified at elevated levels in diabetic tissues [14, 15].

$\alpha$ -Oxoaldehydes are a normal product of metabolism, and cells possess a range of endogenous enzyme systems that ‘detoxify’ these AGE precursors. For example, a glutathione-dependent glyoxalase complex (formed from glyoxalase I [GLO1] and glyoxalase II [GLO2] components) protects cells by converting GO and MG to D-lactate [16]. The capacity of this enzyme system to limit AGEs is demonstrated in endothelial cells which were transfected to overexpress GLO-1 and subsequently showed less accumulation of MG-derived adducts [17]. This was accompanied by protection against high glucose-mediated dysfunction [17, 18]. Overexpression of *GLO1* in diabetic rats has been shown to be protective against AGE formation and oxidative stress in muscle [19], and also prevent abnormalities in endothelium-dependent vasorelaxation [20]. Likewise, regulation of *GLO1* activity in cells can prevent diabetes-related cell dysfunction [21, 22].

MG-derived AGEs are important in diabetic retinopathy. It has been demonstrated that retinal levels of MG-H1 increase by 279% following 24 weeks of diabetes [23], and that MG-H1 correlates with diabetic retinopathy [3]. In retinal cells, MG induces retinal pericyte dysfunction [24] and *GLO1* has been shown to protect against premature death of pericytes and endothelial cells following high glucose exposure [22, 25].

Given that MG-derived adducts are important clinically and that prevention of this pathway has therapeutic potential, we hypothesise that MG-derived AGEs play a key role in neuroglial and microvascular degenerative pathology during the early and intermediate stages of diabetic retinopathy. If this is the case, modulation of the glyoxalase detoxification system could be protective and prevent formation of key retinal lesions during diabetes.

### Methods

**Diabetic rat model** Rats transgenic for human *GLO1* were developed by overexpression of the full-length *GLO1* cDNA under control of the cytomegalovirus enhancer/chicken  $\beta$ -actin promoter system and transgene expression in various tissues was confirmed by PCR. *GLO1*-overexpressing rats were crossed with wild-type (WT) Wistar rats to obtain enough *GLO1* progeny for the experiment. The rats were obtained from the Nippon Seibutsu Zairyo Center (Saitama, Japan) and studies using these animals have been recently published [19, 20]. All

animal studies were carried out in accordance with the Guide for the Care and Use of Laboratory Animals of the National Institutes of Health. All experiments involving rats were reviewed and approved by the Ethics Committee for Animal Care and Use of Maastricht University, the Netherlands.

A total of 55 animals were included in the study (31 WT and 24 *GLO1* rats). At the age of 10 weeks, both rat groups were rendered diabetic by a tail-vein injection of streptozotocin (STZ) (65 mg/kg in citrate buffer for 3 months' duration of diabetes, and 45 mg/kg for 6 months' duration) to prevent severe illness. At 1 and 12 weeks post diabetes induction, blood glucose was measured and only rats with a blood glucose >15 mmol/l at both time points were included in the study. Diabetes was maintained for 3 and 6 months prior to death.

**Rat retinal immunohistology** Eucleated eyes were fixed in 4% paraformaldehyde (PFA) for 30 min, stored in PBS containing 0.1% sodium azide and shipped from the University of Maastricht, the Netherlands to Belfast for investigation. The posterior eye-cup was separated from the globes and the retinas then dissected into two. The half retinas from each sample population were immediately mounted in cryo-embedding compound (BDH, Poole, UK) in a bath of iso-pentane surrounded with dry ice. Samples were stored at  $-20^{\circ}\text{C}$  until used. Prior to sectioning, samples were allowed to equilibrate for approximately 20 min in a cryostat. Retinas were vertically sectioned at 12 or 20  $\mu\text{m}$  and then collected on Superfrost/Plus microscope slides (Menzel-Glaser, Braunschweig, Germany) and stored at  $-20^{\circ}\text{C}$  until use. The other half retinas were used as flat mount preparations (see Staining for acellular capillaries).

Frozen retinal sections were thawed at room temperature and then circled with a DAKO pen (DAKO, Glostrup, Denmark) to provide a barrier for the solutions applied to the sections. They were rehydrated by the application of 200  $\mu\text{l}$  of PBS ( $3 \times 10$  min). Samples were blocked (PBS, pH 7.4, 10% goat serum, 0.1% Triton X-100) for 1 h in a humidity chamber, followed by incubation in a range of primary antibodies including: MG-H1, GLO1 (BioMac, Leipzig, Germany), glial fibrillary acidic protein (GFAP) (Dako), CEL and CML (Cosmobio, Carlsbad, CA, USA), and Kir4.1 (Alomone, Jerusalem, Israel). All primary antibodies were diluted in blocking solution overnight at  $4^{\circ}\text{C}$ . A series of  $4 \times 10$  min washes in PBS was followed by a 1-h incubation at room temperature in an appropriate alexa fluor secondary antibody in the dark (Molecular Probes, Paisley, UK). Sections were washed again  $4 \times 10$  min in PBS and later incubated with DAPI nuclear stain for 5 min, followed by a series of  $3 \times 5$  min washes. Sections were coverslipped with vectashield (Vector Laboratories, Peterborough, UK). Control experiments were

performed by addition of secondary antibody to observe the extent of non-specific antibody binding and secondary antibody autofluorescence.

Fluorescence was either visualised using a Nikon TE-2000 inverted microscope fitted with Nikon C1 confocal system (Nikon, Surrey, UK) or an epi-fluorescence microscope (Nikon Eclipse E400; Nikon). Images were taken from central regions of the retina. For each primary antibody used in the study, the sample with brightest fluorescence was measured first, and confocal settings were held constant when recording images of all subsequent samples. Images were processed and analysed using either ImageJ software (NIH, Bethesda, MD, USA), NIS Elements software (Nikon) or Velocity software (Mountain View, CA, USA). Immunofluorescence was measured by the intensity of the pixels above a threshold, which was defined as 4 SDs above the mean background fluorescence intensity measured from regions devoid of retinal tissue. A user-defined frame was drawn around each layer of the retina and the average fluorescence intensity above the threshold calculated. Either the left or the right eye was analysed for each rat. Six tissue sections were examined per retina.

**Ultra-performance liquid chromatography tandem mass spectrometry analysis** The AGE adducts CML, CEL and MG-H1 were measured in eyes and retina with ultra-performance liquid chromatography tandem mass spectrometry (UPLC-MSMS) as described in detail previously [19]. Liquid chromatography was performed at  $30^{\circ}\text{C}$  using an Acquity UPLC BEH C18, 1.7  $\mu\text{m}$ ,  $2.1 \times 100$  mm column (Waters, Milford, MA, USA), and the Micromass Quattro Premier XE Tandem Mass Spectrometer (Waters) was used in electrospray-positive multiple reaction monitoring mode.

**Quantitative PCR** RNA isolation, reverse transcription and real-time quantitative PCR was performed on retinas isolated from the 3-month experimental groups. The approach was as described previously [26]. Transcripts investigated included *Vegf*, *Tgf $\beta$ -1* and *-2* (also known as *Tgfb1* and *-2*), *Ctgf*, *Icam1*, *Gal3* and *Timp1*.

**Acellular capillary quantification** Retina flat mounts were prepared for immunofluorescence evaluation as previously described [27]. The retinal flat mounts were stained with biotinylated isolectin GS-IB4 overnight (Sigma, Dorset, UK) or for collagen IV immunoreactivity (Acris Antibodies, Germany). Appropriate ligand (streptavidin Alexa Fluor 488) and secondary antibody were used (Alexa Fluor 568 goat anti-rabbit IgG) (both from Molecular Probes). DAPI (Sigma) was also added to visualise the nuclear layers of the retina. Stained retinas were imaged using confocal microscopy (Eclipse TE2000-U; Nikon). Five regions were taken at  $\times 20$  in the central and peripheral retina for collagen IV and lectin.

**Statistical analysis** Data were expressed as the mean values  $\pm$ SEM. Statistical differences in the mean were assessed using the unpaired Student's *t* test or ANOVA. All the statistical analyses were performed using Graph pad InStat 3.0 (GraphPad Software, San Diego, CA, USA).

## Results

**GLO1 expression in rat retina** The diabetic status of these animals has been previously published [19]. The diabetic groups after both time periods were characterised by hyperglycaemia, polydipsia, hyperphagia, polyuria and decreased weight gain, irrespective of their transgenic status. The *GLO1* transgene had no influence on hyperglycaemic status or body weight [19]. *GLO1* activity in various tissues has also been published indicating that there is a significant elevation of functional enzymatic activity when compared with WT controls [19]. The eyes of these animals in particular, demonstrated a  $\sim$ 25-fold increase in *GLO1* activity [19]. *GLO1* immunoreactivity in the retina was markedly elevated in the *GLO1* transgenic rats and was ubiquitously expressed throughout the neural retina (Fig. 1a). Diabetes did not alter the nature of the transgene expression (Fig. 1a–c). The intense immunoreactivity in the

cell bodies of the inner nuclear layer in combination with vertically striated cell localisation from inner to outer retina indicated a high level of Müller glia expression (Fig. 1a). Overall there was no quantitative difference in *GLO1* levels during diabetes, although expression appeared less when *GLO1* rats that had been diabetic for 6 months were compared with those diabetic for 3 months (Fig. 1b and c). This suggests that expression of the transgene was reduced over time or that longer-term diabetes reduced *GLO1* expression.

### *GLO1* overexpression reduces retinal AGEs during diabetes

Various AGE adducts were assessed using a combination of immunohistochemistry and UPLC-MSMS approaches. AGE localisation has been previously demonstrated in the retina and it is established that many of these adducts show a considerable degree of accumulation in Müller glia during diabetes [28–30]. MG-derived CEL has not been previously reported in the retina and this adduct demonstrated increased immunoreactivity in the diabetic retina, even after 3 months of hyperglycaemia, and localisation was in a pattern consistent with Müller glia (Fig. 2a). In diabetic *GLO1* animals, CEL was markedly reduced and localised largely to an astrocyte-like pattern close to the internal limiting membrane (Fig. 2a). Immunolocalisation patterns for each

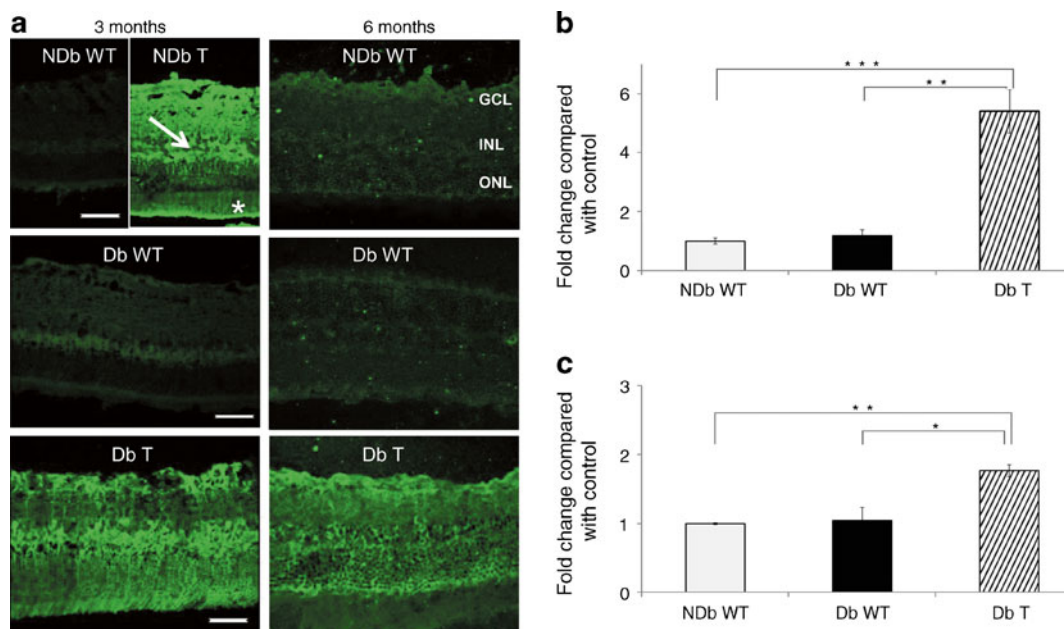


**Fig. 1** GLO1 protein in 3-month and 6-month WT and *GLO1*-transgenic rat retina. **a** Immunofluorescence labelling from non-diabetic wild-type (NDb WT), non-diabetic transgenic (NDb T), diabetic wild-type (Db WT) and diabetic *GLO1* transgenic (Db T) rat retina ( $n \geq 3$ ). Transgenic animals exhibited higher protein levels of GLO1 throughout all layers of the retina (green), although there is particular intensity at the level of the inner nuclear layer (INL), inner limiting membrane (arrow) and external limiting membrane (\*). This demonstrates that the TG animals overexpress *GLO1* in the retina in a

pattern suggesting particularly high levels in the Müller glia. **b** and **c** Quantification of retinal GLO1 protein levels for **(b)** 3- and **(c)** 6-month diabetic rat groups and normalisation to control (NDb WT) levels demonstrates statistical differences between WT and *GLO1* transgenic rat retina. There is no difference in *GLO1* levels between non-diabetic and diabetic WT animals (a–c). Scale bars 50  $\mu$ m, magnification  $\times 40$ , 12  $\mu$ m cryostat sections. GCL, ganglion cell layer; ONL, outer nuclear layer. \* $p < 0.1$ , \*\* $p < 0.01$ , \*\*\* $p < 0.001$



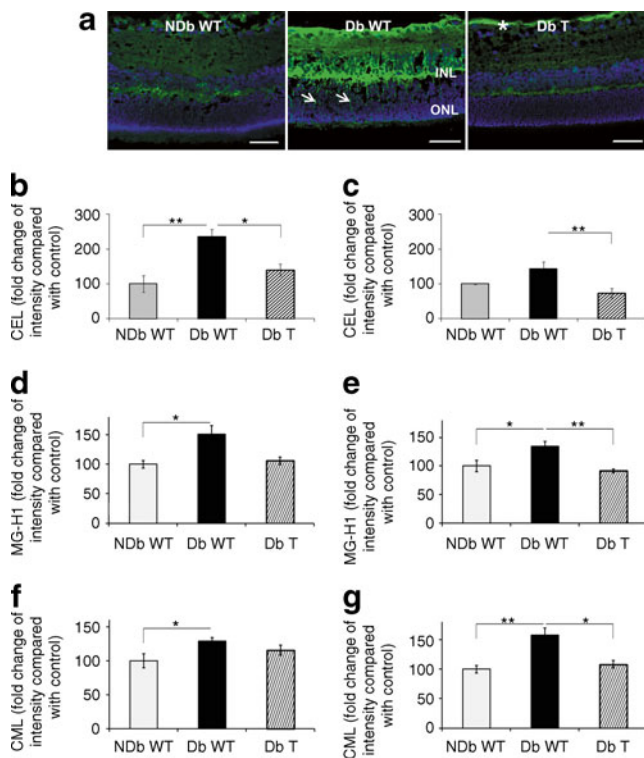


**Fig. 2** AGE immunoreactivity is increased in diabetic retina and are reduced by *GLO1* overexpression. **a** CEL immunoreactivity was markedly increased in the diabetic retina when compared with non-diabetic controls. The localisation pattern of this AGE was consistent with Müller glia showing fluorescence intensity at the inner nuclear layer (INL), inner limiting membrane (arrow) and cytoplasmic processes (arrows) through the outer nuclear layer (ONL). CEL was markedly reduced in diabetic *GLO1* animals and localised largely to an astrocyte-like pattern close to the internal limiting membrane (\*). Scale bars 50  $\mu\text{m}$ , magnification  $\times 40$ . Nuclei counterstained with DAPI. CEL (**b,c**), MG-H1 (**d,e**) and CML (**f,g**) immunoreactivity was quantified in retinal sections at 3 months (**b,d,f**) and 6 months (**c,e,g**). The total intensity of the adducts occurring in the diabetic WT (Db WT) and diabetic *GLO1* transgenic (Db T) rat retinas was analysed and normalised against controls (NDb WT). Diabetic retinas showed higher AGE levels, whereas *GLO1* overexpression reduced the AGE burden in diabetic rats. \* $p < 0.1$ , \*\* $p < 0.01$

of the three AGE adducts (CEL, CML and MG-H1) were similar, and, on quantification, CML and MG-H1 were also significantly increased in the diabetic retina at both 3 and 6 months' post induction ( $p < 0.05$ – $0.01$ ), and presence of the *GLO1* transgene reduced these levels to that of non-diabetic controls (Fig. 2b–g).

AGEs quantified using UPLC-MSMS analysis of whole eye homogenates following 3 or 6 months of diabetes showed a pattern that was comparable with that obtained by immunohistochemistry. There was a significant increase in CEL, MG-H1 and CML in the diabetic retina compared with non-diabetic controls for both 3- and 6-month diabetic animals ( $p < 0.05$ – $0.001$ ). Overexpressing *GLO1* diabetic retina appeared to reduce the accumulation of these AGEs in the

6-month group, although not to levels of the non-diabetic controls (Fig. 3a–f). For animals that were 3 months' diabetic only, it was possible to analyse isolated retina by UPLC-MSMS (electronic supplementary material [ESM] Fig. 1). Although the data did not show significance between the groups, there were apparent trends that corresponded to the retinal immunohistochemistry and whole eye UPLC-MSMS results (compare Figs 2, 3 and ESM Fig. 1).

*GLO1* overexpression prevents Müller glia dysfunction during diabetes In the non-diabetic retina from both WT and *GLO1* rats, GFAP was localised to the astrocytes (Fig. 4a). Diabetes induced a strong upregulation of GFAP in both astrocytes and retinal Müller glia ( $p < 0.05$ ), and there was a small but significant diminution of this protein after 3 months' diabetes in the *GLO1* rats, an effect that became more pronounced after 6 months' diabetes ( $p < 0.05$ – $0.001$ ) (Fig. 4b and c). Another robust diabetes-mediated response by the retinal Müller glia is the mislocalisation of the weakly inward rectifying  $\text{K}^+$  channel Kir 4.1, which is typically localised in Müller glia end-feet and surrounding blood vessels [31]. In diabetic retina, Kir4.1 becomes less localised at the interface with the retinal blood vessels and reduced at the ILM [6, 31]. Following both 3 and 6 months' diabetes, this Kir4.1 response was also observed in the current study (Fig. 5). Overexpression of *GLO1* during diabetes maintained the vascular and Müller glia end-feet localisation (Fig. 5).

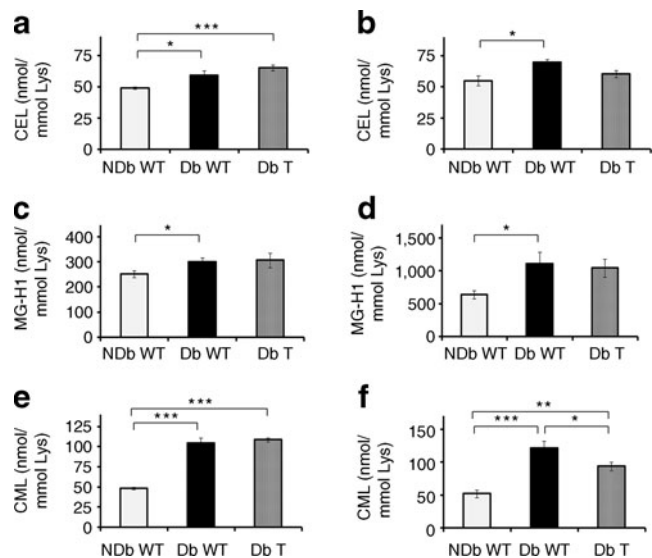


**Fig. 3** AGE quantification in diabetic ocular tissue by UPLC-MSMS. AGEs in whole eye homogenates were analysed using UPLC-MSMS. The levels of CEL (**a,b**), MG-H1 (**c,d**) and CML (**e,f**) show similar trends with enhanced concentrations after 3 months' (**a,c,e**) and 6 months' (**b,d,f**) diabetes compared with non-diabetic controls. *GLO1* overexpressing diabetic animals show reduced AGE levels but only after 6 months. \* $p < 0.05$ ; \*\* $p < 0.01$ ; \*\*\* $p < 0.001$ . Db, diabetic; NDb, non-diabetic; T, transgenic

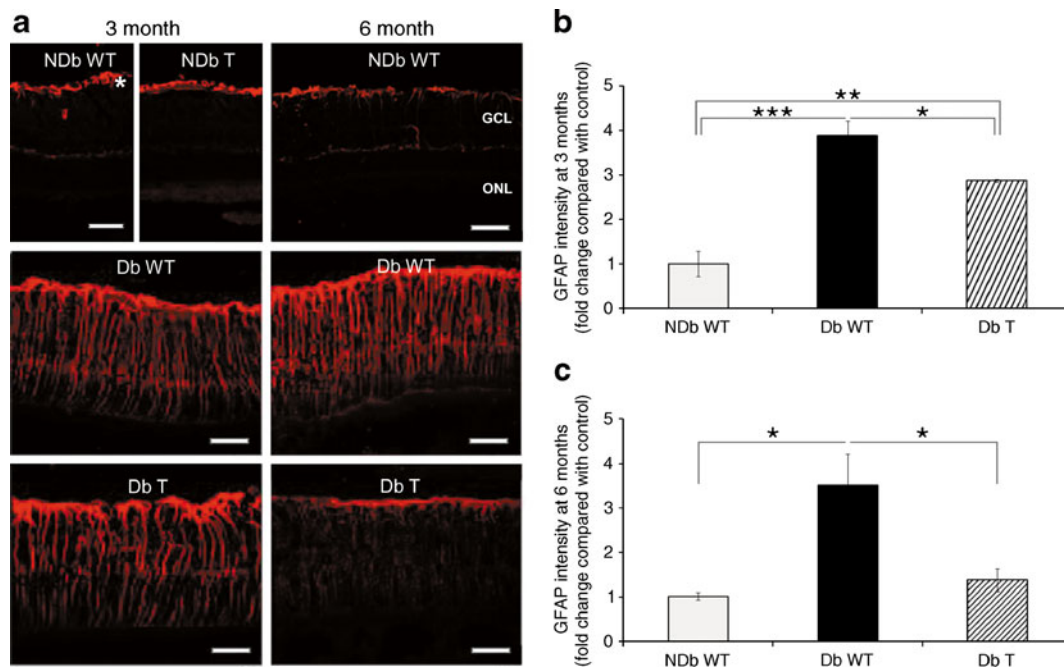


**Fig. 4** *GLO1* regulates GFAP levels in retinal Müller glia during diabetes. **a** GFAP in non-diabetic WT and transgenic rat retina is localised mainly in astrocytes (\*). Following 3 and 6 months of diabetes, GFAP is strongly produced in the retinal Müller glia. Overexpression of *GLO1* reduces this diabetes-mediated response, especially after more prolonged periods of hyperglycaemia. Scale bars 50  $\mu$ m, magnification  $\times 40$ , 12  $\mu$ m cryostat sections. GCL, ganglion cell layer; ONL, outer nuclear layer. **b** and **c** Retinal GFAP levels were

highest in the diabetic WT retina (Db WT) when compared with non-diabetic WT animals (NDb WT). GFAP was significantly reduced in the diabetic *GLO1* transgenic retina (Db T) in both 3-month (**b**) and 6-month (**c**) diabetic groups. No significant differences could be observed between NDb WT and Db T groups in terms of GFAP levels after 6 months. Data were normalised against NDb WT values. \* $p < 0.1$ , \*\* $p < 0.01$ , \*\*\* $p < 0.001$

*GLO1* overexpression in diabetic animals alters retinal expression of key transcripts Quantitative PCR data demonstrated that a range of transcripts was altered during diabetes (Fig. 6). In the WT animals, diabetes induced a significant upregulation of *Gal3*, *Ctgf*, *Timp1* and *Icam1* compared with non-diabetic controls. By contrast, transgenic animals with diabetes did not show this response and it appeared that high *GLO1* attenuated these diabetes-induced responses (Fig. 6). *Vegfa* was not altered by either diabetes or the presence of the *GLO1* transgene. *Tgfb-1* and *-2* mRNA expression was shown to be downregulated in the *GLO1* diabetic retina compared with diabetic WT controls (Fig. 6).

*GLO1* protects against capillary closure Diabetic rats typically show formation of acellular capillaries at around 6 months' post induction [29]. The current study identified collagen IV-positive vascular basement membrane tubes representative of the entire vascular tree in combination with isolectin, which labelled endothelial cells. Strands positive for collagen IV and negative for isolectin indicated acellular capillaries (Fig. 7). Diabetes induced a significant increase in capillary dropout in both the peripheral and central retina, with the latter showing greater levels of pathology (Fig. 7). *GLO1* overexpression in diabetic rats

significantly prevented acellular capillary formation and there were no differences between these treated diabetics in comparison with non-diabetic control groups (Fig. 7).

## Discussion

The relationship between raised intracellular MG, rapid AGE formation and the detoxifying potential of the glyoxalase system has been the focus of intensive study in the area of diabetic complications and ageing [17, 18, 32]. In the context of diabetic retinopathy, the current study has demonstrated that *GLO1* overexpression in diabetic rats prevents hyperglycaemia-induced formation of MG-derived AGEs in the neural retina and prevents Müller glia dysfunction and protects against capillary degenerative pathology. This follows on from previous reports in diabetic rats in which *GLO1* overexpression protected against elevated tissue and systemic circulating levels of AGEs and oxidative stress markers [19], and also prevented hyperglycaemia-mediated impairment of arterial vasorelaxation [20].

Accumulation of AGEs in the diabetic retina is an established phenomenon and their inhibition can effectively prevent key aspects of diabetic retinopathy [8, 9] [33].

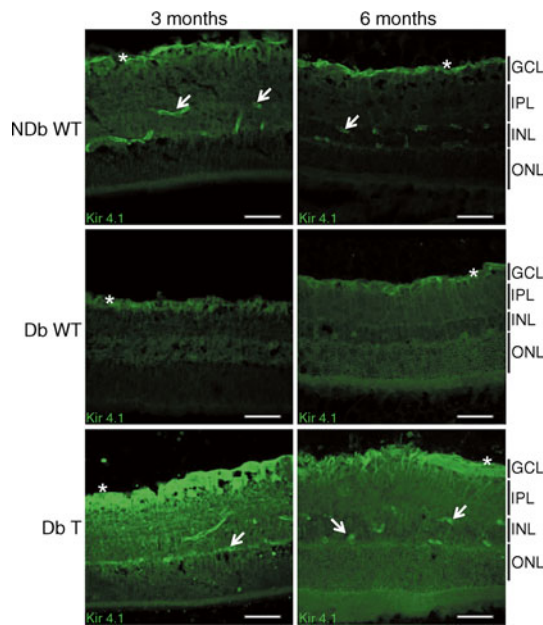


**Fig. 5** Diabetes-mediated mis-localisation of Kir4.1 is prevented by *GLO1* overexpression. In normal retina, the inwardly rectifying channel Kir4.1 (green) is localised at the end-feet of Müller glia at the internal limiting membrane (ILM) (\*) and the perivascular interface (arrows). In diabetic retina, Kir4.1 is no longer visible around the retinal vasculature but is expressed more widely throughout the Müller glia cytoplasm (compare Db WT with the other groups). *GLO1* overexpression in the diabetic retina reduced this diabetes-mediated cellular localisation defect (compare DB T with Db WT). Blue: nuclear stain DAPI, magnification  $\times 20$ , scale bar 100  $\mu\text{m}$ , 20  $\mu\text{m}$  cryostat sections (3 month) and 14  $\mu\text{m}$  sections (6 month). GCL, ganglion cell layer; INL, inner nuclear layer; IPL, inner plexiform layer; ONL, outer nuclear layer

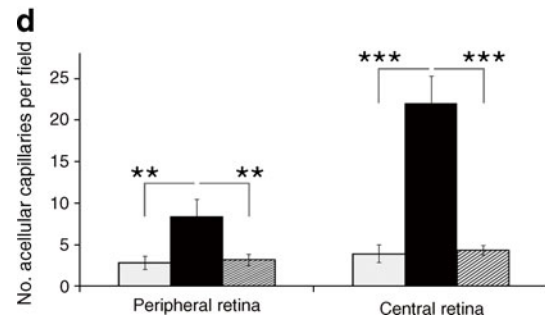
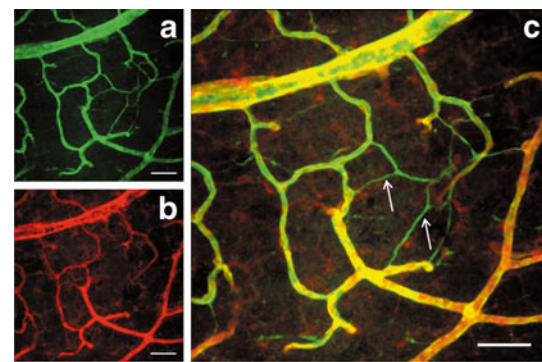


**Fig. 7** *GLO1* overexpression prevents capillary degeneration during diabetic retinopathy. Six months' diabetes causes acellular capillary formation in the retina and this is demonstrated by confocal microscopy of flat-mounted retina. The images show an example of a Db WT retina stained for collagen IV (basement membrane; green) (a) and isolectin (viable endothelium; red) (b). The combined image of (a) and (b) clearly demonstrates the presence of empty basement membranes without endothelial cells, quantified as 'acellular capillaries' (arrows) (c). **d** *GLO1* overexpression in diabetic retinas significantly reduces the amount of acellular capillaries in the peripheral and central retina. Grey bars, NDb WT; black bars, Db WT; hatched bars, Db T. Scale bars 50  $\mu\text{m}$ , magnification  $\times 20$ . \*\* $p < 0.01$ , \*\*\* $p < 0.001$

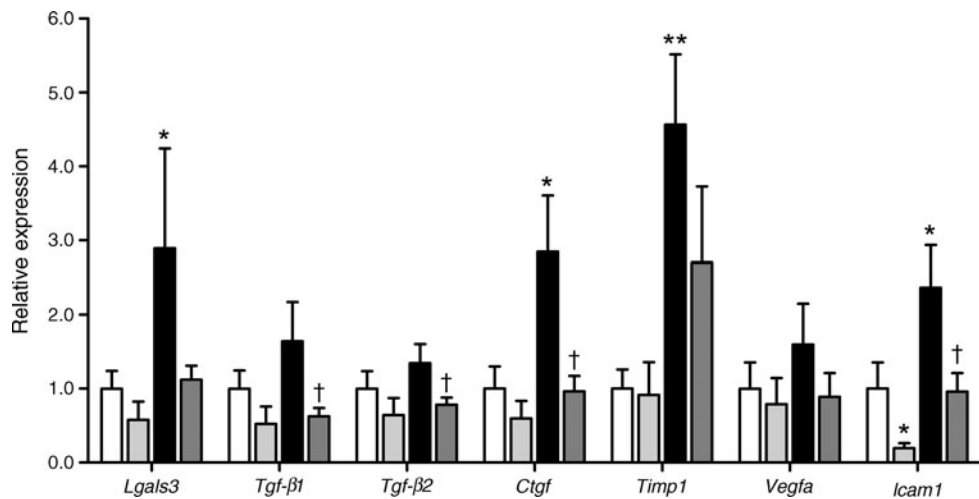


**Fig. 6** Retinal mRNA expression levels of genes regulated during diabetes. The graph shows fold change between the non-diabetic wild-type rats (NDb WT), non-diabetic transgenic *GLO1* rats (NDb T), wild-type rats with 3 months' diabetes (Db WT) and transgenic *GLO1* rats with 3 months' diabetes (Db T). White bars, NDb WT; light grey

bars, NDb T; black bars, Db WT; dark grey bars, Db T. \* $p < 0.05$  for difference between experimental group and NDb WT rats; \*\* $p < 0.01$  for difference between experimental group and NDb WT rats; † $p < 0.05$  for difference between diabetic transgenic and Db WT animals



Although AGEs form in the retina as diabetes progresses, their precise derivation and the relative importance of various adducts remains unclear. The efficacy of benfotiamine in preventing lesions of diabetic retinopathy by addressing hyperglycaemia-mediated oxidative stress and associated elevations of intracellular MG suggests that this  $\alpha$ -oxoaldehyde is an important source of AGEs [11]. To further dissect the importance of MG-derived AGEs in diabetic retinas, the current study has combined immunohistochemistry and UPLC-MSMS to show that CEL, CML and MG-H1 are elevated when compared with non-diabetic controls, and that these adducts appear to accumulate in the retina, particularly in Müller glia. Furthermore, the evidence that *GLO1* overexpression can prevent retinal cell dysfunction and death indicates that MG and GO are not only major precursors for AGEs in the diabetic retina but also that they impact on disease progression.

MG-derived adduct formation also occurs alongside the ‘classic’ Maillard chemistry and other pathways such as myeloperoxidase-mediated protein modification via glycolaldehyde [34], which also contribute to the ‘AGE-load’ during diabetes. However, MG-H1 derived from MG, GO and 3-DG appear to be the major AGEs quantitatively measured in whole retina [23]. It has also been shown that MG-derived adducts accumulate around the retinal blood vessels of diabetic mice [28]. The current study indicates that Müller glia may be an important retinal cell-type for AGE formation in the diabetic retina. In the current study, galectin 3, a protein that binds AGEs and has been shown to be associated with blood retinal barrier dysfunction in diabetes [28], is upregulated in WT diabetic rats. Interestingly, *GLO1* overexpression attenuates this diabetes-induced response. Such data indicate that further studies on the role of *GLO1* in retinal vasopermeability during diabetes are warranted.

A range of AGE adducts may also bind to the receptor for AGEs (RAGE). RAGE is known to be highly expressed by Müller glia in the diabetic retina [30] and, although ligands such as S100B are important in this context, it is possible that receptor activation by MG-derived AGEs could be playing an important role in diabetic retinopathy. Ongoing research is seeking to examine the pathophysiological implications of RAGE and MG-derived AGEs in Müller glia and their contribution to retinal lesions during diabetes.

*GLO1* is part of an enzyme complex that requires reduced glutathione (GSH) as a co-factor and it is possible that following genetic overexpression its detoxification ability would be limited by available GSH. Previous studies have suggested that GSH and oxidised GSH do not change in diabetic retina, although enzymatic activity of superoxide dismutase, glutathione peroxidase, glutathione reductase and glutathione transferase are all reduced in diabetic rats

compared with controls [35]. We have previously published that *GLO1* activity remains high in many tissues of these transgenic rats (including the eye) [19], and the observation that MG-related retinal AGEs are concomitantly reduced suggests that GSH is not limiting in the retina of these transgenic rats.

In addition to the glyoxalase-mediated detoxification, the aldose reductase (AR) pathway also plays a role in regulating intracellular levels of MG [36]. Indeed, MG acts as an aldehyde substrate of AR, which also requires GSH for enzymatic activity [37], although both enzyme systems appear to react differently to the diabetic milieu. For example in diabetic lens, *GLO1* activity goes down, whereas AR is enhanced, and the AGE inhibitor pyridoxamine corrects both these responses [38]. In many tissues where GSH is high and AR activity low, the glyoxalase system may be the main detoxifier of MG [37]. Müller glia contain appreciable levels of intracellular GSH where it has antioxidant activity and is also linked to glutamate transporter activity [39]. Therefore, it is possible that AR and glyoxalase enzymes could both contribute to MG detoxification in the retina. How AR and glyoxalase enzymatic interactions contribute overall to retinal AGEs during diabetes requires further study.

Dysfunction of retinal Müller glia during diabetes has been described previously [31, 40] and manifests as upregulation of GFAP, cytokine expression and impaired protection against retinal excitotoxicity [41–43]. Winkler et al. have demonstrated that Müller glia exposed to high glucose conditions in vitro produce excess lactate, indicative of increased glycolytic flux [44], which would suggest enhanced susceptibility to MG and GO toxicity. In the current study, *GLO1* overexpression protected against changes in GFAP production as a robust stress response by Müller glia associated with AGEs and associated lipid modifications [6]. In addition, *GLO1* overexpression also prevented the diabetes-linked mis-localisation of Kir4.1, which is a phenomenon also impacting on aquaporin 4 channel function in Müller glia [31, 45] and has already been linked to AGE accumulation [6]. Such upset of retinal  $K^+$  clearance and hydration balance could promote oedema and neuronal hyper-excitation as diabetes progresses [31]. Kir4.1 has numerous arginine residues, although it remains unknown if this channel could be directly modified by MG with functional consequences for channel function or its normal association with  $\alpha$ -syntrophin [46].

One of the most significant findings of the current study is that *GLO1* overexpression protects against retinal capillary degeneration over 6 months of diabetes duration. We cannot be definitive if this phenomenon links completely to the observed Müller glia dysfunction established after 3 months of diabetes and ongoing after 6 months. However, such a link would seem likely as these glia play a



major role in vascular integrity in the retina and disruption of the normal vascular-glial interactions, for example in ion exchange at the Müller glia end-feet [45], would impact on capillary degeneration. In addition, the importance of MG in endothelial cell damage during diabetes is established [22] and it has been previously demonstrated that *GLO1* can regulate dysfunction of these cells during high glucose exposure in vitro [17, 18]. In the current in vivo study, it is likely that *GLO1* upregulation maintains the retinal capillary network by a combination of reducing MG-derived AGEs in Müller glia and endothelial cells.

In conclusion, our study demonstrates that elevating *GLO1* offers protection against diabetic retinopathy and the data are consistent with a strong link between elevated MG, AGE formation and cell damage. Recently, it has also been demonstrated that the angiotensin type II receptor inhibitor candesartan can increase *GLO1* activity, prevent formation of MG-derived AGEs and protect against key retinopathic lesions in vivo [47]. Therefore, there is considerable hope that enzymatic detoxification of AGE precursors could be a useful therapeutic target to prevent diabetic complications such as retinopathy.

**Acknowledgements** This work was funded by the Juvenile Diabetes Research Foundation (JDRF), Fight for Sight UK, a Dutch Diabetes Foundation Grant 2005.11.013 and Grant 2005.00.042 from the Diabetes Fonds Nederland. The authors would like to acknowledge the expert technical support of I. Vogels.

**Contribution statement** All authors contributed to analysis and interpretation of data, were involved in drafting the article and approved the final submission. In addition, AWS and CS contributed to the conception and design of the research and directed the overall study.

**Duality of interest** The authors declare that there is no duality of interest associated with this manuscript.

## References

- Stitt AW (2010) AGEs and diabetic retinopathy. *Invest Ophthalmol Vis Sci* 51:4867–4874
- Beisswenger PJ, Szwergold BS, Yeo KT (2001) Glycated proteins in diabetes. *Clin Lab Med* 21:53–78, vi
- Fosmark DS, Torjesen PA, Kilhovd BK et al (2006) Increased serum levels of the specific advanced glycation end product methylglyoxal-derived hydroimidazolone are associated with retinopathy in patients with type 2 diabetes mellitus. *Metabolism* 55:232–236
- Yamaguchi M, Nakamura N, Nakano K et al (1998) Immunochemical quantification of crossline as a fluorescent advanced glycation endproduct in erythrocyte membrane proteins from diabetic patients with or without retinopathy. *Diabet Med* 15:458–462
- Genuth S, Sun W, Cleary P et al (2005) Glycation and carboxymethyllysine levels in skin collagen predict the risk of future 10-year progression of diabetic retinopathy and nephropathy in the diabetes control and complications trial and epidemiology of diabetes interventions and complications participants with type 1 diabetes. *Diabetes* 54:3103–3111
- Curtis TM, Hamilton R, Yong PH et al (2011) Müller glial dysfunction during diabetic retinopathy in rats is linked to accumulation of advanced glycation end-products and advanced lipoxidation end-products. *Diabetologia* 54:690–698
- Stitt AW, Li YM, Gardiner TA, Bucala R, Archer DB, Vlassara H (1997) Advanced glycation end products (AGEs) co-localize with AGE receptors in the retinal vasculature of diabetic and of AGE-infused rats. *Am J Pathol* 150:523–531
- Gardiner TA, Anderson HR, Stitt AW (2003) Inhibition of advanced glycation end-products protects against retinal capillary basement membrane expansion during long-term diabetes. *J Pathol* 201:328–333
- Bhatwadekar A, Glenn JV, Figarola JL et al (2008) A new advanced glycation inhibitor, LR-90, prevents experimental diabetic retinopathy in rats. *Br J Ophthalmol* 92:545–547
- Hammes HP, Alt A, Niwa T et al (1999) Differential accumulation of advanced glycation end products in the course of diabetic retinopathy. *Diabetologia* 42:728–736
- Hammes HP, Du X, Edelstein D et al (2003) Benfotiamine blocks three major pathways of hyperglycemic damage and prevents experimental diabetic retinopathy. *Nat Med* 9:294–299
- Rabbani N, Thornalley PJ (2010) Methylglyoxal, glyoxalase I and the dicarbonyl proteome. *Amino Acids*. doi:10.1007/s00726-010-0783-0
- Kilhovd BK, Giardino I, Torjesen PA et al (2003) Increased serum levels of the specific AGE-compound methylglyoxal-derived hydroimidazolone in patients with type 2 diabetes. *Metabolism* 52:163–167
- Thornalley PJ, Langborg A, Minhas HS (1999) Formation of glyoxal, methylglyoxal and 3-deoxyglucosone in the glycation of proteins by glucose. *Biochem J* 344(Pt 1):109–116
- Glomb MA, Lang G (2001) Isolation and characterization of glyoxal-arginine modifications. *J Agric Food Chem* 49:1493–1501
- Kuhla B, Luth HJ, Haferburg D, Boeck K, Arendt T, Munch G (2005) Methylglyoxal, glyoxal, and their detoxification in Alzheimer's disease. *Ann N Y Acad Sci* 1043:211–216
- Shinohara M, Thornalley PJ, Giardino I et al (1998) Overexpression of glyoxalase-I in bovine endothelial cells inhibits intracellular advanced glycation endproduct formation and prevents hyperglycemia-induced increases in macromolecular endocytosis. *J Clin Invest* 101:1142–1147
- Yao D, Taguchi T, Matsumura T et al (2007) High glucose increases angiotensin-2 transcription in microvascular endothelial cells through methylglyoxal modification of mSin3A. *J Biol Chem* 282:31038–31045
- Brouwers O, Niessen PM, Ferreira I et al (2011) Overexpression of glyoxalase-I reduces hyperglycemia-induced levels of advanced glycation end products and oxidative stress in diabetic rats. *J Biol Chem* 286:1374–1380
- Brouwers O, Niessen PM, Haenen G et al (2010) Hyperglycaemia-induced impairment of endothelium-dependent vasorelaxation in rat mesenteric arteries is mediated by intracellular methylglyoxal levels in a pathway dependent on oxidative stress. *Diabetologia* 53:989–1000
- Bento CF, Fernandes R, Ramalho J et al (2010) The chaperone-dependent ubiquitin ligase CHIP targets HIF-1alpha for degradation in the presence of methylglyoxal. *PLoS One* 5:e15062
- Queisser MA, Yao D, Geisler S et al (2010) Hyperglycemia impairs proteasome function by methylglyoxal. *Diabetes* 59:670–678
- Karachalias N, Babaei-Jadidi R, Ahmed N, Thornalley PJ (2003) Accumulation of fructosyl-lysine and advanced glycation end products in the kidney, retina and peripheral nerve of streptozotocin-induced diabetic rats. *Biochem Soc Trans* 31:1423–1425

24. Denis U, Lecomte M, Paget C, Ruggiero D, Wiernsperger N, Lagarde M (2002) Advanced glycation end-products induce apoptosis of bovine retinal pericytes in culture: involvement of diacylglycerol/ceramide production and oxidative stress induction. *Free Radic Biol Med* 33:236–247
25. Miller AG, Smith DG, Bhat M, Nagaraj RH (2006) Glyoxalase I is critical for human retinal capillary pericyte survival under hyperglycemic conditions. *J Biol Chem* 281:11864–11871
26. Klaassen I, Hughes JM, Vogels IM, Schalkwijk CG, van Noorden CJ, Schlingemann RO (2009) Altered expression of genes related to blood–retina barrier disruption in streptozotocin-induced diabetes. *Exp Eye Res* 89:4–15
27. McVicar CM, Colhoun LM, Abrahams JL et al (2010) Differential modulation of angiogenesis by erythropoiesis-stimulating agents in a mouse model of ischaemic retinopathy. *PLoS One* 5:e11870
28. Canning P, Glenn JV, Hsu DK, Liu FT, Gardiner TA, Stitt AW (2007) Inhibition of advanced glycation and absence of galectin-3 prevent blood–retinal barrier dysfunction during short-term diabetes. *Exp Diabetes Res* 51837:1–10
29. Stitt A, Gardiner TA, Alderson NL et al (2002) The AGE inhibitor pyridoxamine inhibits development of retinopathy in experimental diabetes. *Diabetes* 51:2826–2832
30. Zong H, Ward M, Madden A et al (2010) Hyperglycaemia-induced pro-inflammatory responses by retinal Muller glia are regulated by the receptor for advanced glycation end-products (RAGE). *Diabetologia* 53:2656–2666
31. Pannicke T, Iandiev I, Wurm A et al (2006) Diabetes alters osmotic swelling characteristics and membrane conductance of glial cells in rat retina. *Diabetes* 55:633–639
32. Morcos M, Du X, Pfisterer F et al (2008) Glyoxalase-1 prevents mitochondrial protein modification and enhances lifespan in *Caenorhabditis elegans*. *Aging Cell* 7:260–269
33. Hughes JM, Kuiper EJ, Klaassen I et al (2007) Advanced glycation end products cause increased CCN family and extracellular matrix gene expression in the diabetic rodent retina. *Diabetologia* 50:1089–1098
34. Nagai R, Hayashi CM, Xia L, Takeya M, Horiuchi S (2002) Identification in human atherosclerotic lesions of GA-pyridine, a novel structure derived from glycolaldehyde-modified proteins. *J Biol Chem* 277:48905–48912
35. Obrosova IG, Fathallah L, Greene DA (2000) Early changes in lipid peroxidation and antioxidative defense in diabetic rat retina: effect of DL-alpha-lipoic acid. *Eur J Pharmacol* 398:139–146
36. Aguilera J, Prieto JA (2001) The *Saccharomyces cerevisiae* aldose reductase is implied in the metabolism of methylglyoxal in response to stress conditions. *Curr Genet* 39:273–283
37. Vander Jagt DL, Hassebrook RK, Hunsaker LA, Brown WM, Royer RE (2001) Metabolism of the 2-oxoaldehyde methylglyoxal by aldose reductase and by glyoxalase-I: roles for glutathione in both enzymes and implications for diabetic complications. *Chem Biol Interact* 130–132:549–562
38. Padival S, Nagaraj RH (2006) Pyridoxamine inhibits maillard reactions in diabetic rat lenses. *Ophthalmic Res* 38:294–302
39. Payet O, Maurin L, Bonne C, Muller A (2004) Hypoxia stimulates glutamate uptake in whole rat retinal cells in vitro. *Neurosci Lett* 356:148–150
40. Hammes HP, Federoff HJ, Brownlee M (1995) Nerve growth factor prevents both neuroretinal programmed cell death and capillary pathology in experimental diabetes. *Mol Med* 1:527–534
41. Mizutani M, Gerhardinger C, Lorenzi M (1998) Muller cell changes in human diabetic retinopathy. *Diabetes* 47:445–449
42. Fischer AJ, Scott MA, Ritchey ER, Sherwood P (2009) Mitogen-activated protein kinase-signaling regulates the ability of Muller glia to proliferate and protect retinal neurons against excitotoxicity. *Glia* 57:1538–1552
43. Shelton MD, Kern TS, Mieyal JJ (2007) Glutaredoxin regulates nuclear factor kappa-B and intercellular adhesion molecule in Muller cells: model of diabetic retinopathy. *J Biol Chem* 282:12467–12474
44. Winkler BS, Starnes CA, Sauer MW, Firouzzan Z, Chen SC (2004) Cultured retinal neuronal cells and Muller cells both show net production of lactate. *Neurochem Int* 45:311–320
45. Reichenbach A, Wurm A, Pannicke T, Iandiev I, Wiedemann P, Bringmann A (2007) Muller cells as players in retinal degeneration and edema. *Graefes Arch Clin Exp Ophthalmol* 245:627–636
46. Connors NC, Adams ME, Froehner SC, Kofuji P (2004) The potassium channel Kir4.1 associates with the dystrophin-glycoprotein complex via alpha-syntrophin in glia. *J Biol Chem* 279:28387–28392
47. Miller AG, Tan G, Binger KJ et al (2010) Candesartan attenuates diabetic retinal vascular pathology by restoring glyoxalase-I function. *Diabetes* 59:3208–3215